Effects of Methyl-Substituted Phenanthrolines on the Performance of Ruthenium(II) Dye-Sensitizers

Andressa V. Müller, Poliana S. Mendonça, Stéphane Parant, Thibaut Duchanois, Philippe C. Gros, Marc Beley, André S. Polo

http://dx.doi.org/10.5935/0103-5053.20150208

J. Braz. Chem. Soc., Vol. 26, No. 11, 2224-2232, 2015.
Printed in Brazil - ©2015 Sociedade Brasileira de Química
0103 - 5053 $6.00+0.00

Article

Effects of Methyl-Substituted Phenanthrolines on the Performance of Ruthenium(II) Dye-Sensitizers

Andressa V. Müller,[a] Poliana S. Mendonça,[a] Stéphane Parant,[b,c] Thibaut Duchanois,[b,c] Philippe C. Gros,[b,c] Marc Beley[b,c] and André S. Polo[,a]*

[a]*Universidade Federal do ABC (UFABC), Av. dos Estados, 5001, 09210-170 Santo André-SP, Brazil*

[b]*Université de Lorraine, UMR SRSMC and* [c]*CNRS, UMR SRSMC, HeCRin - Boulevard des Aiguillettes, BP - 54506 Vandœuvre-lès-Nancy, France*

Tris-heteroleptic ruthenium(II) *cis*-[Ru(Me_4-phen)($dcbH_2$)$(NCS)_2$], where Me_4-phen = 3,4,7,8-tetramethyl-1,10-phenanthroline, $dcbH_2$ = 4,4'-dicarboxylic acid 2,2'-bipyridine, was synthesized, purified and characterized. Its characteristics were compared with those determined for *cis*-[Ru(Me_2-phen)($dcbH_2$)$(NCS)_2$] and *cis*-[Ru(phen)($dcbH_2$)$(NCS)_2$] aiming to evaluate the effect of the number of methyl groups on the properties of the compounds. Changes in the Fourier transform infrared (FTIR) and ^{1}H nuclear magnetic resonance (NMR) spectra indicated a modification in the electronic distribution of the complex because of the presence of methyl groups at the 3 and 8 positions of 1,10-phenanthroline. These changes also modified the excited state properties and resulted in a blue shift of the absorption and emission spectra. The complex was incorporated onto TiO_2 to prepare dye-sensitized solar cells, achieving up to J_{SC} = 11.9 mA cm^{-2}, V_{OC} = 0.627 V, ff = 0.67 and η = 5.0%.

Keywords: ruthenium(II) polypyridyl dyes, dye-sensitized solar cells, energy conversion

Introduction

The annual world energy consumption reached 5.5×10^{20} J in 2010, and it is expected to reach 8.7×10^{20} J in 2040 as result of population and economic growth.[1,2] The main sources responsible for the world's energetic needs are liquid fuels, coal and natural gas, which have several disadvantages because they are not renewable and because they emit large quantities of pollutants to the atmosphere.[3] For these reasons, the conversion of solar energy is extremely attractive due to its low environmental impact, infinite supply of energy and its straightforward use in remote areas.[4] Dye-sensitized solar cells (DSSCs) are capable of directly converting sunlight into electricity, and so they could potentially fulfill the world's energy needs. Thus, these devices have attracted considerable attention in recent years.[5-16]

The dye sensitizer is the component responsible for harvesting the sunlight and initiating the energy conversion process. Currently, ruthenium polypyridyl *tris*-heteroleptic compounds are being investigated as dye sensitizers, among other compounds, and have been recently reviewed.[4] These complexes usually contain a bipyridine ligand having carboxylic acid groups, which are responsible for its chemical attachment to the TiO_2 surface, and isothiocyanate ligands are responsible to tune the t_{2g} energy levels of the complex.[13,17] The two remaining coordination sites can be used to coordinate other ligands, with an aim to improve the light absorption or reduction of electron recombination processes. The main compounds that have been investigated are those having bipyridine derivatives, and only a few papers have reported the use of phenanthroline and their derivatives for this purpose. The similarity of phenanthroline to the bipyridyl ligand, coupled with its extended π-conjugated structure, enabled phenanthroline derivatives to be employed in the preparation of dye-sensitizers.[18] The first compound having 1,10-phenanthroline as an ancillary ligand developed for DSSCs demonstrated its potential as a new class of sensitizers.[19] Aiming to improve the performance of this class of compounds, the ancillary ligand was changed to 5,6-dimethyl-1,10-phenanthroline, which exhibited a lower conversion efficiency.[20] Subsequently, this lower efficiency was ascribed to the compound's interfacial electron

*e-mail: andre.polo@ufabc.edu.br

recombination processes.[21] The use of 4,7-diphenyl-1,10-phenanthroline resulted in a complex capable of performing the solar-to-electricity conversion better than the standard compound, $(TBA)_2$*cis*-$[Ru(dcbH)_2(NCS)_2]$, N719.[10]

A possible way to enhance the solar-to-electrical energy conversion is through the use of electron donating groups.[22,23] In a previous work, we investigated the effect of electron donating (i.e., methyl) or withdrawing (i.e., phenyl) substituents on the 4 and 7 positions of 1,10-phenanthroline.[22] In this work, the synthesis and characterization of the new dye *cis*-$[Ru(Me_4\text{-phen})(dcbH_2)(NCS)_2]$ (Me_4-phen = 3,4,7,8-tetramethyl-1,10-phenanthroline; $dcbH_2$ = 4,4'-dicarboxylic acid 2,2'-bipyridine) is described. In addition, the photoelectrochemical performance of this compound as a dye-sensitizer for solar cells is presented and compared with the performance of complexes that possess 4,7-dimethyl-1,10-phenanthroline (Me_2-phen) and 1,10-phenanthroline (phen), which enables us to evaluate the effect of methyl groups on the 3 and 8 positions of the 1,10-phenanthroline ligand.

Experimental

4,4'-Dicarboxylic acid-2,2'-bipyridine (Strem, 99%); $[Ru(p\text{-cymene})Cl_2]_2$ (Strem, 98%); 3,4,7,8-tetramethyl-1,10-phenanthroline, Me_4-phen (Aldrich, 98%); 4,7-dimethyl-1,10-phenanthroline, Me_2-phen (Alfa Aesar, 98%); 1,10-phenanthroline, phen (Strem, 99%); methanolic solution of tetrabutylammonium hydroxide (Acros Organics); Sephadex LH20 (Aldrich); tetrabutylammonium hexafluorophosphate ($TBAPF_6$) (Fluka, ≥ 99.0%); *N*,*N*'-dimethylformamide-d_7, (Aldrich); NaNCS (Merck); HCl (Fluka); HNO_3 (Sigma-Aldrich); methanol (Synth); ethanol (Synth); *N*,*N*-dimethylformamide (DMF) (Synth); Ti-nanoxide T/SP ink (Solaronix); fluorine-doped tin oxide (FTO); conductive glass plates (TEC Glass-TEC 8, solar 2.3 mm thickness 2 × 2 cm); the low temperature sealant Surlyn (30 mm, Solaronix); Pt ink (Platisol, Solaronix); acetonitrile (Lichrosolv, Merck); and Iodolyte AN50-electrolyte (consisting of 0.05 mol L^{-1} of triodide, 0.1 mol L^{-1} of LiI, 0.5 mol L^{-1} of 1,2-dimethyl-3-propylimidazolium iodide and 0.5 mol L^{-1} of 4-*tert*-butylpyridine in acetonitrile, Solaronix) were used as received.

Methods

Nuclear magnetic resonance (NMR) spectra were recorded at 25.0 °C on a DRX-500 Bruker Avance spectrometer at 500.13 MHz using DMF-d_7 as the solvent. The residual DMF peaks were used as an internal standard. Fourier transform infrared (FTIR) spectra were recorded at 25.0 °C in KBr pellets on a Bomem MB 100 spectrometer (with 4 cm^{-1} resolution). Electronic absorption spectra of the complexes fully protonated with HNO_3 were recorded on an Agilent 8453 diode-array spectrophotometer using quartz cuvettes with a 1.000 cm path length. Uncorrected emission spectra were recorded on a Cary Eclipse spectrofluorimeter using quartz cuvettes with a 1.000 cm path length after the samples had been purged with argon. Cyclic voltammetry experiments were performed with a μautolab III potentiostat/galvanostat (Autolab) using a three electrode arrangement comprised of a glassy carbon, platinum and Ag wires as the working, auxiliary and pseudo-reference electrodes, respectively. $TBAPF_6$ was used as the supporting electrolyte dissolved in acetonitrile. The ferrocene/ferrocenium pair was used as the internal standard. Potentials were reported *versus* the normal hydrogen electrode (NHE) using $E_{1/2}$ (Fc/Fc^+) = 0.67 V *vs.* NHE.[24]

Fabrication of the dye-sensitized solar cells

A sandwich-type cell was assembled from a transparent photosensitive electrode, a platinum coated electrode and an I^-/I_3^- based electrolyte. Titania films (0.6 × 0.6 cm^2) were obtained by the screen-printing technique using Ti-nanoxide T/SP ink on FTO conductive glass plates. First, the TiO_2 film was dried at 150 °C for 10 min and then heated under an air atmosphere at 450 °C for 30 min. The thickness of the transparent TiO_2 layer was measured at 8 μm. The film was then immersed overnight in a 0.5 mmol L^{-1} dye solution and a 5 mmol L^{-1} chenodeoxycholic acid solution in methanol/acetonitrile 1:1 (v:v). Then, the electrode was rinsed with solvent before assembly with the counter electrode. A thin Pt layer was used as the counter electrode, which was also prepared by screen-printing Pt ink onto the FTO coated glass substrate and then heated at 450 °C for 30 min under an air atmosphere. The platinum counter electrode and the dye-adsorbed TiO_2 electrode were assembled together by heating at 110 °C a hot-melt film sandwiched between the two electrodes. Then, the Iodolyte AN50-electrolyte was filled between the two electrodes with a syringe. The reproducibility of the DSSC preparation was controlled by preparing three replicates and by performing various tests as described below.

Photoelectrochemical measurements

The spectral response was determined by measuring the wavelength dependence of the incident photon-to-current conversion efficiency (IPCE) using light from

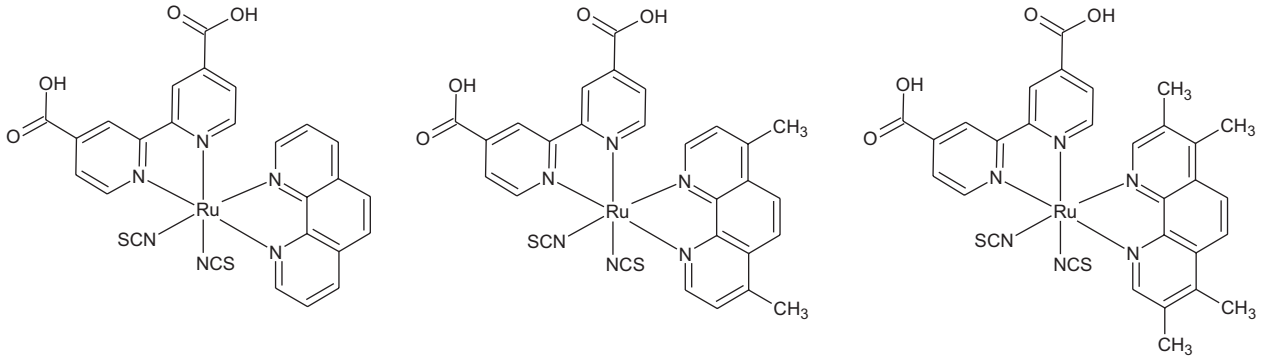

Figure 1. Chemical structures of *cis*-[Ru(phen)($dcbH_2$)$(NCS)_2$], *cis*-[Ru(Me_2-phen)($dcbH_2$)$(NCS)_2$] and *cis*-[Ru(Me_4-phen)($dcbH_2$)$(NCS)_2$].

an Osram 300-W xenon lamp coupled to a Newport monochromator (Oriel Cornerstone 260). Photocurrents were measured under short circuit conditions (in DC mode) using a Newport 1936R instrument. Incident irradiance was measured with a 1 cm^2 calibrated silicon photodiode. Current-voltage characteristics were determined by applying an external potential bias using a Radiometer PGP 201 potentiostat sweeping the potential with a scan rate of 10 mV s^{-1}. The irradiation source was a Solaronix Luminox A lamp, which matches the AM 1.5 (100 mW cm^{-2}) solar spectrum. Incident irradiance was measured with an ISO-Tech ISM410. The cell temperature was kept below 30 °C. The data were averaged for three cells for each configuration.

Synthesis of *cis*-[Ru(R_n-phen)($dcbH_2$)$(NCS)_2$]

The *cis*-[Ru(Me_4-phen)($dcbH_2$)$(NCS)_2$], *cis*-[Ru(Me_2-phen)($dcbH_2$)$(NCS)_2$] and *cis*-[Ru(phen)($dcbH_2$)$(NCS)_2$] complexes, Figure 1, were prepared by a one-pot procedure, as previously reported.[22] Briefly, the ruthenium *p*-cymene dimer, [Ru(*p*-cymene)$Cl_2]_2$, was added to *N*,*N*'-dimethylformamide (DMF) and 2 equivalents of R_n-phen were then added. The mixture was kept at 80 °C for 2 h under an inert atmosphere. After this period, 2 equivalents of $dcbH_2$ were added to the mixture, and the temperature was increased to 160 °C. The mixture was kept at this temperature for 4 h. Finally, a 10-fold excess of NaNCS was added to the mixture, the temperature was decreased to 140 °C and the reaction was kept under these conditions for 4 h, allowing it to proceed to completion. All reactions were monitored by UV-Vis spectrophotometry. To purify the compounds, the obtained solution was concentrated, washed and filtered with ultrapure H_2O, diluted in methanol and deprotonated by using a basic methanolic solution, obtained by dilution of tetrabutylammonium hydroxide (1 mol L^{-1}), and centrifuged to remove any residual particles. The solution was applied to a liquid column chromatography containing Sephadex LH-20 as the stationary phase and methanol as the eluent. The pure fraction was concentrated, precipitated by the addition of HNO_3 and filtered. The solid was dried in a desiccator. Using this procedure, it was possible to synthesize *cis*-[Ru(Me_4-phen)($dcbH_2$)$(NCS)_2$] (yield 51%; anal. calcd. for $C_{30}H_{30}N_6O_7RuS_2$: C, 47.93; H, 4.02; N, 11.18%. Found: C, 49.46; H, 4.33; N, 10.86%), *cis*-[Ru(Me_2-phen)($dcbH_2$)$(NCS)_2$] (yield 70%; anal. calcd. for $C_{28}H_{24}N_6O_6RuS_2$: C, 46.47; H, 3.62; N, 11.61. Found: C, 48.71; H, 4.04; N, 11.47%) and *cis*-[Ru(phen)($dcbH_2$)$(NCS)_2$] (yield 78%; anal. calcd. for $C_{26}H_{21}N_6O_7RuS_2$: C, 44.83; H, 3.49; N, 12.31. Found: C, 44.95; H, 3.05; N, 12.10%).

Results

FTIR spectroscopy

Typical signals of functional groups are observed in the FTIR spectrum for *cis*-[Ru(Me_4-phen)($dcbH_2$)$(NCS)_2$], Figure 2. The CH bond bending of the aromatic rings (1940-1915 cm^{-1} region), the methyl groups (1462, 1384 and 1367 cm^{-1}) and the OH of the carboxylic acids (1425 and 1407 cm^{-1}) can be observed. In addition to the signals described previously, it is important to note the ν_{CO}

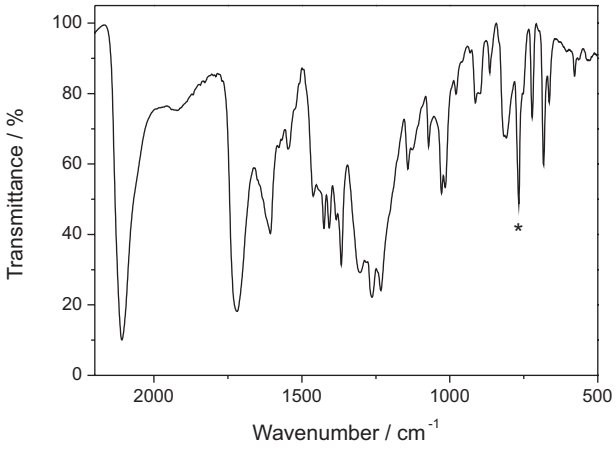

Figure 2. FTIR spectrum of *cis*-[Ru(Me_4-phen)($dcbH_2$)$(NCS)_2$] in KBr. (* indicates the peak ascribed to the –NCS ligand at 768 cm^{-1}).

stretching of the carboxylic groups (1720 cm^{-1}) and the ν_{CN} of the NCS^- ligand (2109 and 768 cm^{-1}).

The $\nu_{CN(NCS)}$ signals observed with FTIR are also a useful tool to verify the existence of NCS^- linkage isomers. The existence of these peaks indicates the coordination of this ligand by the nitrogen atom, as is described for other compounds.[22] The typical peak of NCS^- coordination through the sulfur atom can be typically observed at 2050 and 700 cm^{-1}.[14] However, they are not observed in the present spectrum. Thus, it is possible to conclude that the isothiocyanate complex is the only isomer obtained after purification.

^{1}H NMR spectroscopy

^{1}H-^{1}H COSY was used to assign the protons signals of *cis*-[Ru(Me_4-phen)($dcbH_2$)$(NCS)_2$] to the respective ligand, $dcbH_2$ or Me_4-phen, Figure 3. Because the protons were assigned, NMR spectroscopy allowed an evaluation for the electronic influence of the substituents on the chemical shifts and proton couplings determined by the ^{1}H NMR spectrum, Table 1. The number of signals observed in the ^{1}H spectrum is consistent with the *cis* configuration of the complex, which reduces its symmetry and results in non-equivalent protons.

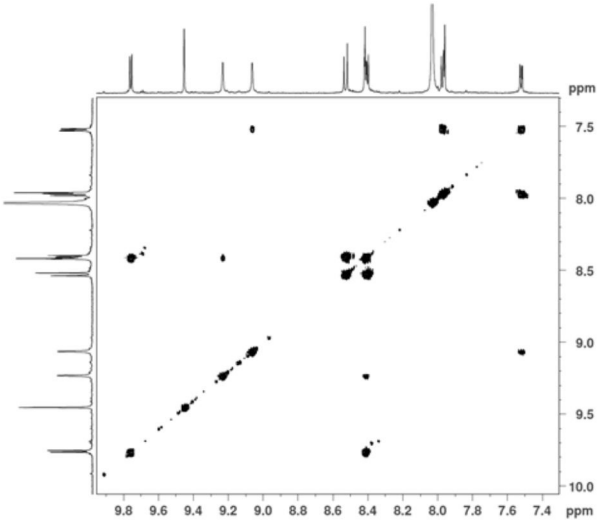

Figure 3. ^{1}H-^{1}H COSY of *cis*-[Ru(Me_4-phen)($dcbH_2$)$(NCS)_2$] in DMF-d_7. (T = 298 K; 500 MHz).

The signals corresponding to the Me_4-phen ligand are consistent with the proposed structure (Figure 1), exhibiting only one proton coupling between H_5 and H_6. For the H_2 and H_9 protons, a difference in their chemical shifts is observed relative to the values reported for *cis*-[Ru(Me_2-phen)($dcbH_2$)$(NCS)_2$]. The chemical shift values for *cis*-[Ru(Me_4-phen)($dcbH_2$)$(NCS)_2$] are

Table 1. Chemical shifts and proton couplings determined for *cis*-[Ru(Me_4-phen)($dcbH_2$)$(NCS)_2$] in DMF-d_7 (500 MHz, T = 298 K)

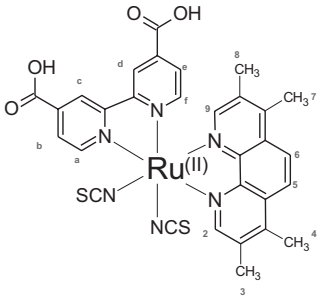

	Proton type	δ / ppm	J / Hz
	H_a (d, 1H)	9.76	5.8
	H_b (d, 1H)	8.42	5.8
	H_c (s, 1H)	9.23	–
	H_d (s, 1H)	9.06	–
	H_e (d, 1H)	7.56	6.0
	H_f (d, 1H)	7.97	6.0
	H_2 (s, 1H)	9.45	–
	H_3 (s, 3H)	3.00	–
	H_4 (s, 3H)	2.78	–
	H_5 (d, 1H)	8.53	9.4
	H_6 (d, 1H)	8.40	9.4
	H_7 (s, 3H)	2.73	–
	H_8 (s, 3H)	2.29	–
	H_9 (s, 1H)	7.96	–

9.58 and 8.50 ppm, whereas the analogous values for *cis*-[Ru(phen)($dcbH_2$)$(NCS)_2$] are 9.74 and 8.19 ppm.[22] These differences indicate an electronic influence of the methyl group on these protons.

Electrochemistry

Electrochemical parameters of the complexes *cis*-[Ru(Me_4-phen)($dcbH_2$)$(NCS)_2$], *cis*-[Ru(Me_2-phen)($dcbH_2$)$(NCS)_2$] and *cis*-[Ru(phen)($dcbH_2$)$(NCS)_2$] were determined by using cyclic voltammetry in acetonitrile, Figure 4.

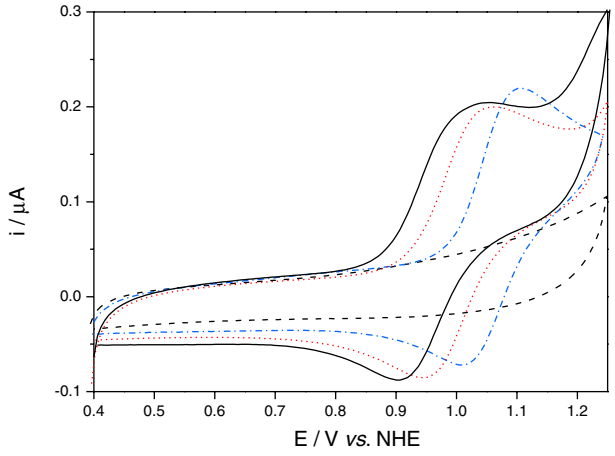

Figure 4. Cyclic voltammograms of *cis*-[Ru(Me_4-phen)($dcbH_2$)$(NCS)_2$] (–), *cis*-[Ru(Me_2-phen)($dcbH_2$)$(NCS)_2$] (····) and *cis*-[Ru(phen)($dcbH_2$)$(NCS)_2$] (·–·–) in acetonitrile (---) at 293 K (v = 100 mV s^{-1}; [$TBAPF_6$] = 0.1 mol L^{-1}).

The cyclic voltammograms exhibit a *quasi*-reversible oxidation process for the ruthenium(II/III) wave for

cis-[Ru(Me_4-phen)($dcbH_2$)($NCS)_2$], *cis*-[Ru(Me_2-phen)($dcbH_2$)($NCS)_2$] and *cis*-[Ru(phen)($dcbH_2$)($NCS)_2$], having $E_{1/2}$ = 0.98, 1.01 and 1.05 V *vs.* NHE, respectively. The $E_{1/2}$ for *cis*-[Ru(phen)($dcbH_2$)($NCS)_2$] is in agreement with the value reported in the literature.[19]

Absorption spectrum

The electronic spectrum of *cis*-[Ru(Me_4-phen)($dcbH_2$)($NCS)_2$] in acetonitrile, Figure 5, exhibits high energy absorption bands (up to 350 nm), which are ascribed to intraligand π-π* transitions of the Me_4-phen and $dcbH_2$ ligands. Absorption bands with maxima at 420 nm (1.3×10^4 L mol^{-1} cm^{-1}) and at 535 nm (0.8×10^4 L mol^{-1} cm^{-1}) are observed in the visible region of the spectrum, which overlap the sunlight spectrum. The high molar absorptivities determined for this compound indicate the presence of MLCT transitions, as has been described in the literature for similar compounds.[10,25] The existence of these absorption bands increases the sunlight harvesting by this compound.

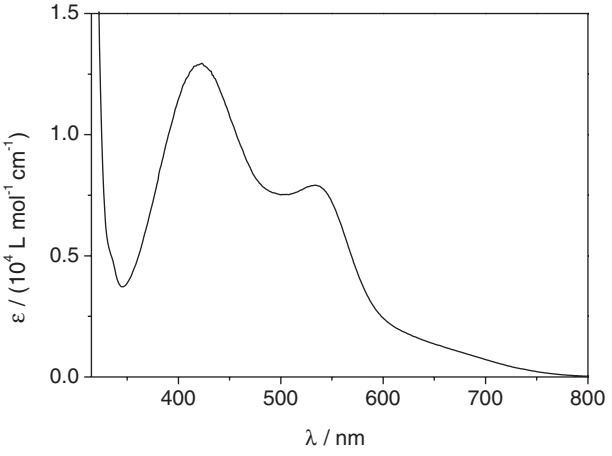

Figure 5. Electronic spectrum of *cis*-[Ru(Me_4-phen)($dcbH_2$)($NCS)_2$] in acetonitrile.

The features of the absorption spectrum, as well as the absorption maxima and molar absorptivity, are similar to the data reported for *cis*-[Ru(Me_2-phen)($dcbH_2$)($NCS)_2$] (ε_{430nm} = 1.3×10^4 L mol^{-1} cm^{-1}) and *cis*-[Ru(phen)($dcbH_2$)($NCS)_2$] ($\varepsilon_{420nm} = 1.2 \times 10^4$ L mol^{-1} cm^{-1}).[22]

Emission spectrum

The emission spectrum of *cis*-[Ru(Me_4-phen)($dcbH_2$)($NCS)_2$] in acetonitrile, Figure 6, is broad and non-structured, exhibiting an intense emission maximum at 800 nm. The emission feature and its maximum are typical of a ^{3}MLCT lowest lying excited state of ruthenium polypyridyl compounds.[26]

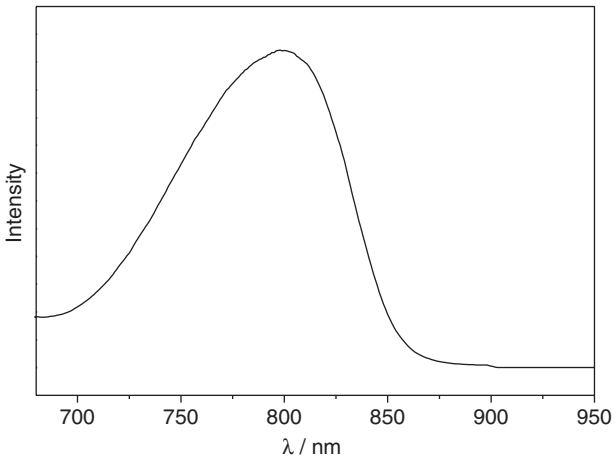

Figure 6. Emission spectrum of *cis*-[Ru(Me_4-phen)($dcbH_2$)($NCS)_2$] in acetonitrile at T = 293 K (λ_{ex} = 500 nm; v = 30 nm min^{-1}).

The estimated HOMO-LUMO energy gap, $E_{0\text{-}0}$, determined for the complexes is 1.81 eV for *cis*-[Ru(Me_4-phen)($dcbH_2$)($NCS)_2$], 1.84 eV for *cis*-[Ru(Me_2-phen)($dcbH_2$)($NCS)_2$] and 1.92 eV for *cis*-[Ru(phen)($dcbH_2$)($NCS)_2$]. These values were determined at the onset of the optical emission spectrum. The excited state oxidation potentials, $E(S^+/S^*)$, were calculated by using the equation $E(S^+/S^*) = E_{1/2}(S/S^+) - E_{0\text{-}0}$,[10] where $E_{1/2}(S/S^+)$ is the ground state oxidation potential determined by cyclic voltammetry, Table 2.

Photoelectrochemical measurements

The sensitization of TiO_2 films was monitored up to 14 h by absorption changes on the visible region, Figure 7. These absorption changes occur due to the increase in dye loading, which is responsible for the sensitization, following the MLCT band of each dye along the time. It is

Table 2. Emission maxima wavelength, λ_{em}, estimated HOMO-LUMO energy gaps, $E_{0\text{-}0}$, ground state oxidation potentials, $E_{1/2}(S^+/S)$, and excited state oxidation potentials, $E(S^+/S^*)$, for the compounds investigated

Sensitizer	λ_{em} / nm	$E_{0\text{-}0}$ / eV	$E_{1/2}(S^+/S)$ / V *vs.* NHE	$E(S^+/S^*)$ / V *vs.* NHE
cis-[Ru(Me_4-phen)($dcbH_2$)($NCS)_2$]	800	1.81	0.98	–0.83
cis-[Ru(Me_2-phen)($dcbH_2$)($NCS)_2$]	805	1.84	1.01	–0.83
cis-[Ru(phen)($dcbH_2$)($NCS)_2$]	790	1.92	1.05	–0.87

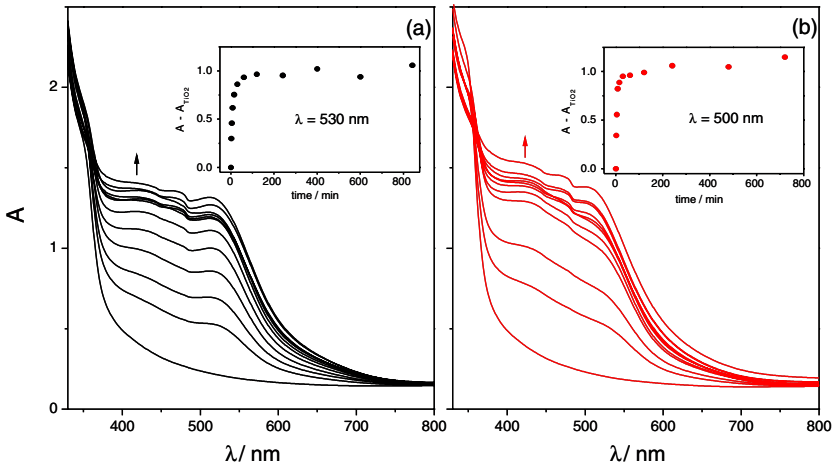

Figure 7. Absorption spectra of TiO_2 films being sensitized by *cis*-[Ru(Me_4-phen)($dcbH_2$)($NCS)_2$] (a); or *cis*-[Ru(Me_2-phen)($dcbH_2$)($NCS)_2$] (b). (Insets: absorption changes as a function of time).

important to notice the absence of shifts on the absorption maxima indicating that a dye monolayer was adsorbed onto TiO_2. The amount of dye-loaded was evaluated by their desorption from the film after full loading, and are 9.0×10^{-8}, 11×10^{-8} and 9.0×10^{-8} mol cm^{-2}, respectively for *cis*-[Ru(Me_4-phen)($dcbH_2$)($NCS)_2$], *cis*-[Ru(Me_2-phen)($dcbH_2$)($NCS)_2$] and *cis*-[Ru($dcbH)_2(NCS)_2]^{2-}$ (N719), which was used as a standard for comparison.

Dye sensitized solar cells were assembled using TiO_2 sensitized films and solar cells were characterized by photocurrent action spectra and current-voltage curves. The photocurrent action spectra establish a relationship between the photocurrent generated by the incident light at a determined wavelength and the light intensity, thus it is possible to access information of the efficiency of the dye at each wavelength. Additionally, important photoelectrochemical parameters from solar cells, such as open-circuit potential, V_{OC}, short circuit current density, J_{SC}, and the overall performance of the solar cell, η, can be determined by the current-voltage curves, which are accessed by exposing the DSSC to simulated solar irradiation.[4]

The photocurrent action spectra of *cis*-[Ru(Me_4-phen)($dcbH_2$)($NCS)_2$], *cis*-[Ru(Me_2-phen)($dcbH_2$)($NCS)_2$] and *cis*-[Ru($dcbH)_2(NCS)_2]^{2-}$, Figure 8, resemble the absorption spectra of the respective dye-sensitized TiO_2 and show that these compounds are capable of harvesting the sunlight and converting it into electrical energy in the visible region of the spectrum.

The spectral features of *cis*-[Ru(Me_4-phen)($dcbH_2$)($NCS)_2$] and *cis*-[Ru(Me_2-phen)($dcbH_2$)($NCS)_2$] are similar, and the spectra of both are different than the standard N719 in the 350-400 nm region. A lower efficiency can also be observed for the *cis*-[Ru(Me_4-phen)($dcbH_2$)($NCS)_2$] dye relative to *cis*-[Ru(Me_2-phen)($dcbH_2$)($NCS)_2$] for the entire spectrum. Dye-sensitized solar cells prepared by using these

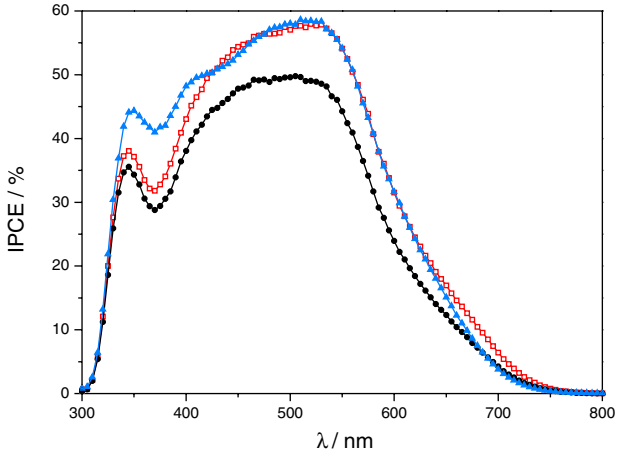

Figure 8. Photocurrent action spectra of *cis*-[Ru(Me_4-phen)($dcbH_2$)($NCS)_2$] (●), *cis*-[Ru(Me_2-phen)($dcbH_2$)($NCS)_2$] (□) and *cis*-[Ru($dcbH)_2(NCS)_2]^{2-}$ (▲).

complexes are able to convert the sunlight into electricity, and their performances were evaluated by JV curves, Figure 9, and their photoelectrochemical parameters are listed in Table 3.

As was expected on the basis of the photocurrent action spectra, a lower J_{SC} is determined for *cis*-[Ru(Me_4-phen)($dcbH_2$)($NCS)_2$] in comparison to *cis*-[Ru(Me_2-phen)($dcbH_2$)($NCS)_2$] and N719, resulting in the lowest overall efficiency determined for *cis*-[Ru(Me_4-phen)($dcbH_2$)($NCS)_2$] by JV curves.

Discussion

The FTIR spectrum of the compound demonstrates the predominance of isothiocyanate because the typical peaks of the thiocyanate isomer are not observed. The presence of the linkage isomer coordinated by the sulfur atom exhibits a ν_{SCN-} at 2050 cm^{-1} and a resonance at 700 cm^{-1}.[14]

Table 3. Photoelectrochemical parameters determined for *cis*-[Ru(Me_n-phen)($dcbH_2$)($NCS)_2$], n = 2 or 4 and for *cis*-[Ru($dcbH)_2(NCS)_2]^{2-}$, N719

	cis-[Ru(Me_4-phen)($dcbH_2$)($NCS)_2$]	*cis*-[Ru(Me_2-phen)($dcbH_2$)($NCS)_2$]	N719
V_{OC} / V	0.627	0.637	0.687
J_{SC} / (mA cm^{-2})	11.9	13.7	13.25
η / %	5.0	5.9	6.1
Fill factor	0.67	0.67	0.67

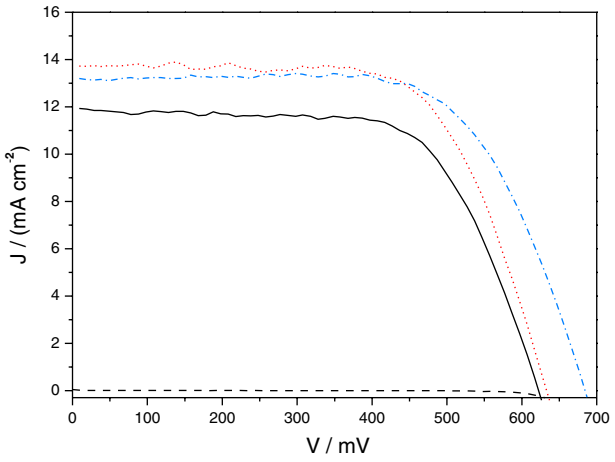

Figure 9. Current – voltage curves determined for *cis*-[Ru(Me_4-phen)($dcbH_2$)($NCS)_2$] (–), *cis*-[Ru(Me_2-phen)($dcbH_2$)($NCS)_2$] (····) and *cis*-[Ru($dcbH)_2(NCS)_2]^{2-}$ (····) under AM 1.5 irradiation (P = 100 mW cm^{-2}) and for *cis*-[Ru($dcbH)_2(NCS)_2]^{2-}$ in the dark (---).

Additionally, the use of ^{1}H NMR spectroscopy indicates the presence of only one isomer and confirms the existence of the *cis*-complexes. This is evident because the number of signals observed in the spectrum is consistent with the existence of non-equivalent protons for the *cis*-isomer. A comparison of the *cis*-[Ru(Me_4-phen)($dcbH_2$)($NCS)_2$] FTIR data to those reported for *cis*-[Ru(Me_2-phen)($dcbH_2$)($NCS)_2$][22] indicates the electronic influence of the methyl groups at the 3 and 8 positions on the NCS^- stretching mode (2109 cm^{-1}), which is shifted by −8 cm^{-1} relative to *cis*-[Ru(Me_2-phen)($dcbH_2$)($NCS)_2$]. This result indicates a reduction of the electronic density on the NCS^- ligand.

Changes of the electronic density on the metal center also shift the redox potential of the ruthenium(II/III) process to lower potentials. A more pronounced shift was observed as the number of methyl groups increases, which suggests that the electronic density on the metal center has increased. Changes to the ruthenium(II/III) $E_{1/2}$ value as a function of the nature of the phenanthroline substituents are described for several ruthenium compounds[27-29] and can be predicted by using ligand electrochemical parameters.[30]

The oxidation potentials of the excited states of *cis*-[Ru(Me_n-phen)($dcbH_2$)($NCS)_2$], n = 2 or 4, are more negative than the conduction band edge of TiO_2 anatase (E_{CB} = –0.4 V *vs.* NHE),[10] and their ground state oxidation potentials are more positive than the $I_2^{-\bullet}/I^-$ (+0.93 V *vs.* NHE)[31] redox pair, Figure 10. The energy of these components is adequate for their use in dye-sensitized solar cells because they permit the electron to move from the excited state of the complexes into the conduction band of TiO_2. Thermodynamically, their subsequent regeneration by the redox pair is favorable.

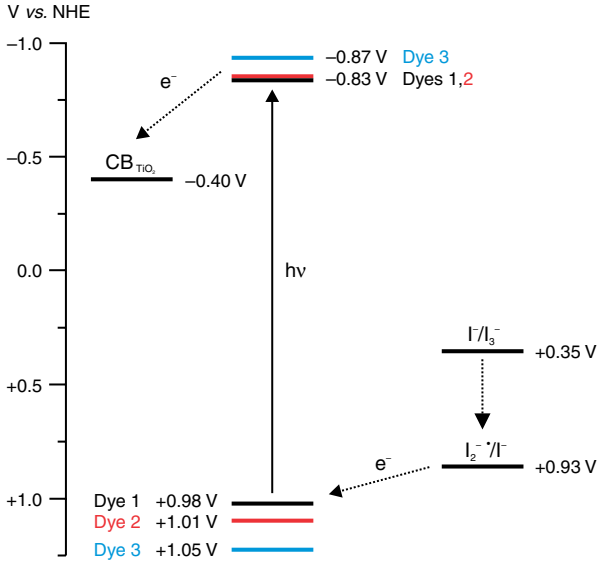

Figure 10. Energy diagram for the dyes (**1**) *cis*-[Ru(Me_4-phen)($dcbH_2$)($NCS)_2$]; (**2**) *cis*-[Ru(Me_2-phen)($dcbH_2$)($NCS)_2$] and (**3**) *cis*-[Ru(phen)($dcbH_2$)($NCS)_2$].

The number of methyl groups on 1,10-phenanthroline changes the electronic distribution of the excited state and has an impact on the electronic spectrum of *cis*-[Ru(Me_4-phen)($dcbH_2$)($NCS)_2$], which resembles those determined for similar complexes.[10,19,22] However, its molar absorptivity in the visible light region (450-600 nm) is lower than that observed for similar compounds where the solar spectral irradiance is at a maximum. Its emission spectrum exhibits a maximum at 800 nm, which is blue shifted by 5 nm relative to *cis*-[Ru(Me_2-phen)($dcbH_2$)($NCS)_2$]. This result indicates a destabilization of the ^{3}MLCT excited state and is responsible for the emission detected.

The photoelectrochemical performance of *cis*-[Ru(Me_4-phen)($dcbH_2$)($NCS)_2$] reflects the changes to the ground

and excited states. The presence of four methyl groups on 1,10-phenanthroline reduces its solar light harvesting capacity and destabilizes the ^{3}MLCT excited state. Consequently, its performance is lower than that reported for *cis*-[Ru(Me_2-phen)($dcbH_2$)($NCS)_2$] but is similar to *cis*-[Ru(phen)($dcbH_2$)($NCS)_2$].[22] Thus, the presence of four electron donating groups attached to phenanthroline does not improve the solar-to-electrical energy conversion. IPCE values determined for *cis*-[Ru(Me_4-phen)($dcbH_2$)($NCS)_2$] are lower than those of *cis*-[Ru(Me_2-phen)($dcbH_2$)($NCS)_2$] along the entire spectrum, which is consistent with its JV performance. The same trend is observed for the J_{SC} values, as determined by JV curves, which is primarily responsible for the lower energy conversion efficiency of this compound.

The lower photocurrent determined for *cis*-[Ru(Me_4-phen)($dcbH_2$)($NCS)_2$] relative to *cis*-[Ru(Me_2-phen)($dcbH_2$)($NCS)_2$] can be ascribed to the lower solar light harvesting capacity of the former complex. The dye regeneration dynamics must also be considered to explain the differences observed on the overall cell efficiencies. Since the ground state redox potentials are not positive enough to access the $I^{\bullet}/I^-$ (1.23 V *vs.* NHE), the regeneration mechanism is expected to proceed by $I_2^{-\bullet}/I^-$ pathway,[31,32] Figure 10. The driving force of electron transfer from mediator to *cis*-[Ru(Me_4-phen)($dcbH_2$)($NCS)_2$] is lower than to *cis*-[Ru(Me_2-phen)($dcbH_2$)($NCS)_2$], indicating that the less favorable regeneration process reduces the cell efficiency. The lower efficiency observed can also be due to a higher recombination rate of the injected electron to the oxidized dye. This process reduces both the J_{SC} and V_{OC} values,[33,34] as was observed in this case. *cis*-[Ru(Me_4-phen)($dcbH_2$)($NCS)_2$] exhibits a V_{OC} value that is 10 mV lower than the same value for *cis*-[Ru(Me_2-phen)($dcbH_2$)($NCS)_2$], indicating that the recombination process can also reduce the efficiency of energy conversion. If this is the case, the methyl groups at the 3 and 8 positions play an important role in the back electron transfer processes for dye-sensitized solar cells. In this respect, further investigations are being performed on the recombination processes.

Conclusions

The new *cis*-[Ru(Me_4-phen)($dcbH_2$)($NCS)_2$] dye-sensitizer was prepared and characterized. Its characteristics were compared to *cis*-[Ru(Me_2-phen)($dcbH_2$)($NCS)_2$] and *cis*-[Ru(phen)($dcbH_2$)($NCS)_2$] to evaluate the influence of methyl groups at the 3 and 8 positions of the phenanthroline ligand. This compound exhibits a wide overlap to the visible spectrum, it sensitizes the TiO_2 film and it is able to convert the sunlight into electrical energy in dye-sensitized solar cells. The presence of the four methyl groups on 1,10-phenanthroline leads to changes in both the ground and excited states of the complex. Overall, this changes reduces the solar light harvesting capacity of the complex and destabilizes its ^{3}MLCT excited state. Consequently, its efficiency as a sensitizer is lower than that reported for *cis*-[Ru(Me_2-phen)($dcbH_2$)($NCS)_2$], which is consistent with the lower IPCE values along the entire spectrum and the JV performance. The lower photocurrent can be ascribed to the lower solar light harvesting capacity of *cis*-[Ru(Me_4-phen)($dcbH_2$)($NCS)_2$], to dye regeneration dynamics or to a higher recombination rate of the injected electron to the oxidized dye, which is ascribed to a reduction of the J_{SC} and V_{OC} values, indicate that the methyl groups at the 3 and 8 positions play an important role in back electron transfer processes for dye-sensitized solar cells.

Acknowledgements

A. V. Müller and A. S. Polo are grateful to Fundação de Amparo à Pesquisa do Estado de São Paulo (FAPESP) for financial support (2013/25173-5 and 2015/00605-5). M. B. and P. C. G. are grateful for support from the Université de Lorraine and CNRS. IS2-SAS is also gratefully acknowledged for providing a grant to T. D.

References

1. Reynal, A.; Palomares, E.; *Eur. J. Inorg. Chem.* **2011**, 4509.
2. Gratzel, M.; *Inorg. Chem.* **2005**, *44*, 6841.
3. Souza, S. S.; Patrocinio, A. O. T.; *Quim. Nova* **2014**, *37*, 886.
4. de Souza, J. S.; de Andrade, L. O. M.; Polo, A. S. In *Nanoenergy*; de Souza, F. L.; Leite, E. R., eds.; Springer: Heidelberg, 2013, p. 49.
5. Bignozzi, C. A.; Argazzi, R.; Boaretto, R.; Busatto, E.; Carli, S.; Ronconi, F.; Caramori, S.; *Coord. Chem. Rev.* **2013**, *257*, 1472.
6. Caramori, S.; Cristino, V.; Boaretto, R.; Argazzi, R.; Bignozzi, C. A.; Di Carlo, A.; *Int. J. Photoenergy* **2010**, 16.
7. O'Regan, B. C.; Durrant, J. R.; *Acc. Chem. Res.* **2009**, *42*, 1799.
8. Ghosh, B.; Naskar, S.; Naskar, S.; Espinosa, A.; Hau, S. C. K.; Mak, T. C. W.; Sekiya, R.; Kuroda, R.; Chattopadhyay, S. K.; *Polyhedron* **2014**, *72*, 115.
9. Ludin, N. A.; Mahmoud, A.; Mohamad, A. B.; Kadhum, A. A. H.; Sopian, K.; Karim, N. S. A.; *Renewable Sustainable Energy Rev.* **2014**, *31*, 386.
10. Sun, Y. L.; Onicha, A. C.; Myahkostupov, M.; Castellano, F. N.; *ACS Appl. Mater. Interfaces* **2010**, *2*, 2039.
11. Siu, C. H.; Ho, C. L.; He, J.; Chen, T.; Majumda, P.; Zhao, J. Z.; Li, H.; Wong, W. Y.; *Polyhedron* **2014**, *82*, 71.

12. Urbani, M.; Medel, M.; Kumar, S. A.; Chandiran, A. K.; Gonzalez-Rodriguez, D.; Gratzel, M.; Nazeeruddin, M. K.; Torres, T.; *Polyhedron* **2014**, *82*, 132.
13. Li, G.; Hu, K.; Robson, K. C. D.; Gorelsky, S. I.; Meyer, G. J.; Berlinguette, C. P.; Shatruk, M.; *Chem. Eur. J.* **2015**, *21*, 2173.
14. Nazeeruddin, M. K.; Kay, A.; Rodicio, I.; Humphry-Baker, R.; Müller, E.; Liska, P.; Vlachopoulos, N.; Grätzel, M.; *J. Am. Chem. Soc.* **1993**, *115*, 6382.
15. Oregan, B.; Gratzel, M.; *Nature* **1991**, *353*, 737.
16. Zakeeruddin, S. M.; Nazeeruddin, M. K.; Humphry-Baker, R.; Pechy, P.; Quagliotto, P.; Barolo, C.; Viscardi, G.; Gratzel, M.; *Langmuir* **2002**, *18*, 952.
17. Nazeeruddin, M. K.; Grätzel, M.; *J. Photochem. Photobiol., A* **2001**, *145*, 79.
18. Hara, K.; Sugihara, H.; Tachibana, Y.; Islam, A.; Yanagida, M.; Sayama, K.; Arakawa, H.; Fujihashi, G.; Horiguchi, T.; Kinoshita, T.; *Langmuir* **2001**, *17*, 5992.
19. Onozawa-Komatsuzaki, N.; Kitao, O.; Yanagida, M.; Himeda, Y.; Sugihara, H.; Kasuga, K.; *New J. Chem.* **2006**, *30*, 689.
20. Reynal, A.; Forneli, A.; Martinez-Ferrero, E.; Sanchez-Diaz, A.; Vidal-Ferran, A.; Palomares, E.; *Eur. J. Inorg. Chem.* **2008**, 1955.
21. Reynal, A.; Forneli, A.; Martinez-Ferrero, E.; Sánchez-Díaz, A.; Vidal-Ferran, A.; O'Regan, B. C.; Palomares, E.; *J. Am. Chem. Soc.* **2008**, *130*, 13558.
22. Carvalho, F.; Liandra-Salvador, E.; Bettanin, F.; Souza, J. S.; Homem-de-Mello, P.; Polo, A. S.; *Inorg. Chim. Acta* **2014**, *414*, 145.
23. Beley, M.; Gros, P. C.; *Organometallics* **2014**, *33*, 4590.
24. Crabtree, R. H.; *Energy Production and Storage: Inorganic Chemical Strategies for a Warming World*; Wiley: Singapore, **2013**.
25. Adeloye, A. O.; *Molecules* **2011**, *16*, 8353.
26. Nazeeruddin, M. K.; Zakeeruddin, S. M.; Humphry-Baker, R.; Jirousek, M.; Liska, P.; Vlachopoulos, N.; Shklover, V.; Fischer, C. H.; Grätzel, M.; *Inorg. Chem.* **1999**, *38*, 6298.
27. Guttentag, M.; Rodenberg, A.; Bachmann, C.; Senn, A.; Hamm, P.; Alberto, R.; *Dalton Trans.* **2013**, *42*, 334.
28. Lever, A. B. P.; *Inorg. Chem.* **1990**, *29*, 1271.
29. Nakada, A.; Koike, K.; Nakashima, T.; Morimoto, T.; Ishitani, O.; *Inorg. Chem.* **2015**, *54*, 1800.
30. Fielder, S. S.; Osborne, M. C.; Lever, A. B. P.; Pietro, W. J.; *J. Am. Chem. Soc.* **1995**, *117*, 6990.
31. Boschloo, G.; Hagfeldt, A.; *Acc. Chem. Res.* **2009**, *42*, 1819.
32. da Silva, R.; Rego, L. G. C.; Freire, J. A.; Rodriguez, J.; Laria, D.; Batista, V. S.; *J. Phys. Chem. C.* **2010**, *114*, 19433.
33. O'Regan, B. C.; López-Duarte, I.; Martínez-Díaz, M. V.; Forneli, A.; Albero, J.; Morandeira, A.; Palomares, E.; Torres, T.; Durrant, J. R.; *J. Am. Chem. Soc.* **2008**, *130*, 2906.
34. O'Regan, B. C.; Durrant, J. R.; *Acc. Chem. Res.* **2009**, *42*, 1799.

Submitted: June 24, 2015
Published online: August 21, 2015

FAPESP has sponsored the publication of this article.